

Growing with the Generator: Self-paced GRPO for Video Generation

Rui Li^{1*}, Yuanzhi Liang^{3†}, Ziqi Ni², Haibing Huang³, Chi Zhang³, Xuelong Li^{3‡}

¹University of Science and Technology of China

²Southeast University,

³Institute of Artificial Intelligence (TeleAI), China Telecom

rui.li@mail.ustc.edu.cn, liangyzh18@outlook.com, xuelong.li@ieee.org

Abstract

Group Relative Policy Optimization (GRPO) has emerged as a powerful reinforcement learning paradigm for post-training video generation models. However, existing GRPO pipelines rely on static, fixed-capacity reward models whose evaluation behavior is frozen during training. Such rigid rewards introduce distributional bias, saturate quickly as the generator improves, and ultimately limit the stability and effectiveness of reinforcement-based alignment. We propose Self-Paced GRPO, a competence-aware GRPO framework in which reward feedback co-evolves with the generator. Our method introduces a progressive reward mechanism that automatically shifts its emphasis from coarse visual fidelity to temporal coherence and fine-grained text–video semantic alignment as generation quality increases. This self-paced curriculum alleviates reward–policy mismatch, mitigates reward exploitation, and yields more stable optimization. Experiments on VBench across multiple video generation backbones demonstrate consistent improvements in both visual quality and semantic alignment over GRPO baselines with static rewards, validating the effectiveness and generality of Self-Paced GRPO.

1. Introduction

Video generation with reinforcement learning (RL) has recently attracted growing attention for its ability to align generative models with perceptual and semantic preferences. Different from reconstruction-based methods, RL introduces feedback-driven optimization rather than supervised reconstruction objectives. Among various formulations, Group Relative Policy Optimization (GRPO) has shown strong potential in this domain [19, 34], offering stable optimization and preference-oriented gradients through group-

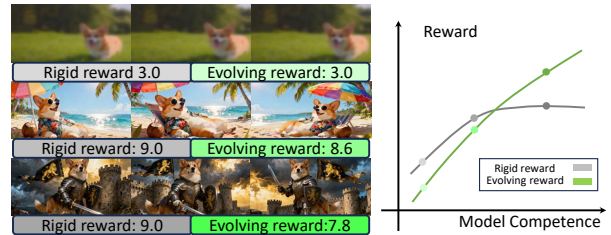


Figure 1. As video quality improves, scores of static reward models may flatten and fail to capture group-level discrimination. In contrast, evolving rewards adapt to the generation competence and remain sensitive to quality gains throughout training.

wise comparisons. Building on this foundation, recent studies have explored improved scheduling, reward shaping, and multimodal feedback strategies [4, 8, 16]. These efforts highlight a consistent finding: the reward model is the central factor in GRPO-based visual generation. It evaluates generation quality and encodes human-aligned preferences, thereby determining overall effectiveness.

Current reward modeling approaches generally follow two paradigms [15, 20, 33]. The first employs lightweight perceptual or image/video-quality assessment (IQA) models adapted from aesthetic or technical benchmarks. These models are efficient but often shallow, encouraging generators to exploit low-level cues. The second leverages visual–language models (VLMs) fine-tuned with human-preference data via RLHF, such as VideoAlign based evaluators. While demonstrating improvements in certain aspects, such models unavoidably inherit distributional biases from training data, over-rewarding specific prompt categories, which can destabilize optimization and lead to reward exploitation during training. Despite their differences, both paradigms share a fundamental limitation: they are static and ability-fixed. Once trained, these rewards remain unchanged throughout optimization, providing identical evaluation signals regardless of the generator’s competence. This rigidity creates a mismatch between reward dif-

*Equal contribution.

†Equal contribution.

‡Corresponding author.

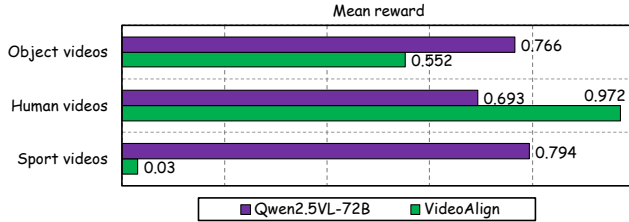


Figure 2. Illustration of reward model bias. VideoAlign shows content-specific preference, often assigning higher scores to certain video categories.

ficulty and model ability—weak models are over-penalized by strong gradients, whereas strong ones quickly saturate and gain diminishing effective guidance. These observations suggest that the core issue lies in the lack of adaptability in current reward modeling. Then a natural question arises: why not allow the reward itself to grow with the generative model, enabling it to provide increasingly challenging and meaningful feedback as the model improves?

In this paper, we propose **Self-Paced GRPO** for video generation. As shown in Fig. 1, the core concept is that reward supervision should evolve alongside the generator’s competence rather than remain static during training. We design a co-evolving reward mechanism that dynamically adjusts evaluation difficulty as generation quality improves, encouraging the model to progress through increasingly challenging objectives while maintaining stable optimization. Grounded in principles of hierarchical and adaptive learning [3, 7, 14, 28], our approach treats reward adaptation as an implicit curriculum. Specifically, we introduce a three-stage reward structure: the first stage emphasizes coarse visual fidelity and aesthetic appeal, the second incorporates temporal consistency and motion coherence, and the final stage enforces text–video alignment to ensure semantic accuracy and realistic dynamics. This hierarchical supervision enables the generator and reward model to co-evolve, mitigating bias, reducing capacity mismatch, and stabilizing policy optimization across training stages.

Our main contributions are summarized as follows:

Self-Paced GRPO for Video Generation. We present a GRPO framework that adaptively scales reward signals according to the generator’s competence, reducing generator-reward mismatch and bias in existing RL-based generation pipelines.

Co-Evolving Reward Mechanism. We propose a progressive, three-stage reward model that evolves from coarse visual supervision to fine-grained temporal and semantic alignment, enabling structured and stable learning.

Improved Preference Alignment. Extensive experiments demonstrate consistent gains in visual quality, temporal coherence, and text alignment compared with existing baselines.

2. Related Work

Post Training of Visual Synthesis. Early efforts in optimizing visual synthesis primarily relied on Proximal Policy Optimization (PPO) [6]. These methods first trained a value network to capture specific human preferences, then used the trained reward model to score the generated videos, and performed preference fine-tuning based on these scores. However, PPO-based approaches require maintaining a value network, which leads to low training efficiency. Building upon this idea, Group Relative Policy Optimization [19, 29, 34] extends preference optimization to multi-modal generative tasks. By leveraging group-based relative comparisons rather than single-sample rewards, GRPO can capture richer preference signals and achieve more robust alignment in visual synthesis models.

Multi-Stage Approaches. Multi-stage optimization has been widely adopted to progressively refine generative models across spatial, temporal, and semantic dimensions. For example, Spatial-then-temporal [17] first enhance spatial and appearance features using static images, and then incorporate temporal information through video reconstruction with a distillation loss to preserve spatial representations. TTC [21] improve spatial quality via masked region restoration and subsequently enhance temporal consistency with a three-frame sampling strategy and an auxiliary branch. Enhance-A-Video [22] further enhance temporal consistency by emphasizing off-diagonal elements in the temporal attention map and scaling cross-frame attention values. These studies highlight the potential of multi-stage design in post-training for video generation. They inspire us to structure training into distinct stages, each targeting a specific dimension.

Reward Models. Recent studies [6, 10] have introduced IQA models and VLMs as reward functions, enabling semantically grounded reinforcement learning for visual generation. For instance, VILA [18] has been applied to construct preference pairs for human alignment [36], while VideoAlign [23] is employed to enhance both visual quality and motion quality in text-to-video generation [34]. As shown in Fig. 2, such VLMs inevitably inherit biases from the training data, leading to preferences for certain types of video content. Similarly, InFLVG [4] leverages frame-wise consistency and CLIP-based similarity to facilitate coherent long-form video generation. Despite these advances, they implicitly assume that the generator and the reward model are well matched in capability. In practice, however, the supervision strength of a fixed reward model is often misaligned, either too weak or overly strong, resulting in unstable training. Moreover, relying on a single reward model renders these methods vulnerable to reward hacking. To mitigate this, VRG [24] leverage diverse reward models (e.g., CLIP [25], HPSv2 [32], and other vision-language or video representation models [1, 5, 27, 30]) to jointly opti-

mize semantic alignment, perceptual quality, and temporal coherence. Nevertheless, jointly employing multiple reward models may lead to conflicts among them, and balancing the supervision strength across different reward models also remains challenging.

3. Preliminary

SDE Sampling. In ODE sampling, the sampling process is deterministic, formulated as

$$dx_t = v_t dt, \quad (1)$$

where v_t denotes the control variable at time t , without any stochastic component.

However, since reinforcement learning requires stochasticity to encourage exploration, such a deterministic model is not sufficiently flexible for exploration in GRPO. Unlike ODE sampling, which follows a single deterministic trajectory, SDE sampling introduces stochastic perturbations that encourage exploration and prevent collapse to suboptimal modes. It incorporates both a drift term and a diffusion term.

$$dx_t = \underbrace{\left(v_t(x_t) - \frac{\sigma^2}{2} \nabla \log p_t(x_t) \right)}_{\text{drift term}} dt + \underbrace{\sigma_t dw}_{\text{diffusion term}}, \quad (2)$$

where the *drift term* governs the deterministic dynamics of the process, while the *diffusion term* introduces stochastic perturbations through Brownian motion, thereby enhancing exploration.

Coefficient of Variation. The coefficient of variation κ is a normalized measure of dispersion, defined as the ratio of the standard deviation to the mean of a dataset. Unlike raw variance or standard deviation, κ provides a scale-independent metric, making it suitable for comparing variability across datasets with different units or magnitudes. A lower κ indicates that the data points are relatively consistent around the mean, while a higher κ suggests greater relative variability. κ is widely used in statistics and experimental analysis to assess stability, reliability, and the degree of heterogeneity in observations.

Formally, suppose the dataset is partitioned into clusters, where s_{ij} denotes the score of the j -th video in the i -th cluster, and each cluster contains N videos. The mean, standard deviation, and coefficient of variation κ for the i -th cluster are computed as:

$$\kappa_i = \frac{\left(\frac{1}{N} \sum_{j=1}^N (s_{ij} - \mu_i)^2 \right)^{1/2}}{\frac{1}{N} \sum_{j=1}^N s_{ij}} \times 100\%. \quad (3)$$

4. Method

In reinforcement-based video generation, static reward models often fail to capture group-level discrimination, losing effectiveness once the generator surpasses their reward

capacity, leading to reward saturation and unstable optimization. To address this issue, the proposed Self-Paced GRPO framework integrates a Co-Evolving Reward Mechanism (CERM) into the Group Relative Policy Optimization paradigm. The reward evolves jointly with the generator’s competence, defined as its ability to produce high-quality samples under the current reward. This formulation creates a continuous curriculum of learning signals, ensuring adaptability and robustness across diverse data distributions.

4.1. Co-Evolving Reward

Let $v_i = \{f_t^i\}_{t=1}^T$ denote a sampled video with T frames. For optimization, we consider groups of size G . A collection of latent reward terms $\{\varphi_j(\cdot)\}_{j=1}^K$ is defined, each capturing a distinct aspect of generation quality. For term j , the scalar reward is

$$r_j^i = \varphi_j(v_i), \quad \mathbf{r}_j = (r_j^1, r_j^2, \dots, r_j^G). \quad (4)$$

The overall reward is modeled as a competence-dependent mixture of these terms:

$$\tilde{r}_i = \sum_{j=1}^K w_j r_j^i, \quad \sum_{j=1}^K w_j = 1, \quad w_j \in [0, 1], \quad (5)$$

where c denotes the generator’s current competence level. The weighting function employs a soft selection strategy,

$$w_j = \frac{\exp(\alpha g_j(c, \mathbf{r}_j))}{\sum_{\ell=1}^K \exp(\alpha g_\ell(c, \mathbf{r}_\ell))}, \quad (6)$$

where $g_j(\cdot)$ indicates the contribution of each reward term and α controls transition sharpness. This continuous formulation removes discrete stage boundaries and allows the reward to evolve smoothly with model improvement, aligning supervision difficulty with the generator’s competence.

4.2. Competence-Aware Reward Adaptation

Competence is estimated from group-relative reward statistics. For each reward term, the mean reward is

$$\bar{r}_j = \frac{1}{G} \sum_{i=1}^G r_j^i, \quad (7)$$

and a reward sparsity is measured using the Hoyer index [9]:

$$S_{\text{Hoyer}}(\mathbf{r}_j) = \frac{\sqrt{G} - \frac{\|\mathbf{r}_j\|_1}{\|\mathbf{r}_j\|_2}}{\sqrt{G} - 1}, \quad S_{\text{Hoyer}}(\mathbf{r}_j) \in [0, 1]. \quad (8)$$

A high sparsity value indicates reward saturation, implying that most samples receive similar scores. The transition function coupling competence and sparsity is defined as

$$g_j(c, \mathbf{r}_j) = h(\bar{r}_j - \tau_j) + \beta [S_{\text{Hoyer}}(\mathbf{r}_{j-1}) - S_{\text{Hoyer}}(\mathbf{r}_j)], \quad (9)$$

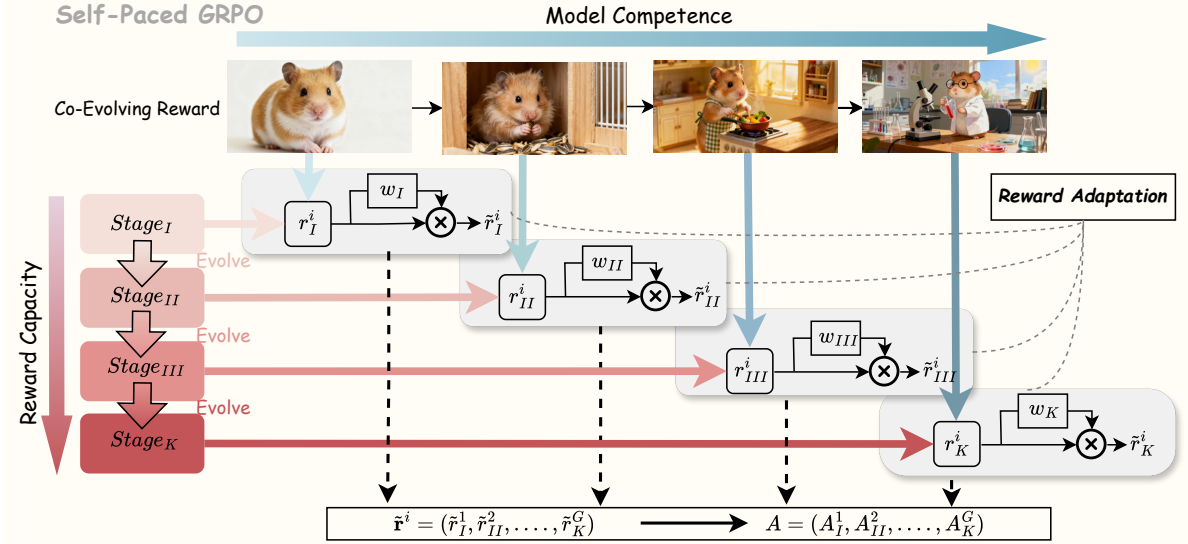


Figure 3. Pipeline of the proposed Self-Paced GRPO. The generator produces candidate outputs, which are evaluated by a progressive co-evolving reward mechanism. Rewards are aggregated and gated through a competence-aware adaptation strategy, enabling adaptive stage-wise aggregation. The normalized reward feedbacks are then used to compute advantages that guide gradient-based fine-tuning of the generator.

where $h(\cdot)$ is a smooth activation (sigmoid), τ_j is a competence threshold, and β balances sparsity modulation. A higher mean reward and stronger sparsity signal that the current reward term is saturated, prompting a gradual transition toward more advanced reward terms. This adaptive weighting process parallels curriculum and self-paced learning, enabling the generator to progress from coarse to fine-grained supervision in a stable and continuous manner.

4.3. Self-Paced GRPO

The generalized mechanism can be instantiated with three reward terms of increasing abstraction. The first emphasizes structural regularity and visual coherence. The second incorporates temporal dependency, promoting smooth motion evolution. The third enforces semantic alignment between generated content and conditioning signals. During training, the thresholds $\{\tau_j\}$ are calibrated empirically, and all reward terms are precomputed once per group to ensure unbiased comparison. This hierarchical progression follows the principles of progressive representation learning, supporting a smooth transition from low-level regularities to structured temporal and semantic reasoning.

Reward Normalization and Advantage Computation. To ensure stability and comparability across groups, the evolving reward is standardized before policy optimization:

$$A_i^{\text{CERM}} = \frac{\tilde{r}_i - \text{mean}(\tilde{\mathbf{r}})}{\text{std}(\tilde{\mathbf{r}})}. \quad (10)$$

Normalization enforces scale invariance and prevents extreme samples from dominating optimization. The normal-

ized advantage provides a consistent and stable signal for policy improvement under evolving reward supervision.

Training Objective. The final optimization objective extends standard GRPO by incorporating the co-evolving reward:

$$\mathcal{J}(\theta) = \mathbb{E}_{\substack{\{\mathbf{o}_i\}_{i=1}^G \sim \pi_{\theta_{\text{old}}}(\cdot|\mathbf{c}) \\ \mathbf{a}_{t,i} \sim \pi_{\theta_{\text{old}}}(\cdot|\mathbf{s}_{t,i})}} \left[\frac{1}{G} \sum_{i=1}^G \frac{1}{T} \sum_{t=1}^T \min(\rho_{t,i} A_i^{\text{CERM}}, \text{clip}(\rho_{t,i}, 1 - \epsilon, 1 + \epsilon) A_i^{\text{CERM}}) \right], \quad (11)$$

where $\rho_{t,i} = \frac{\pi_{\theta}(a_{t,i}|\mathbf{s}_{t,i})}{\pi_{\theta_{\text{old}}}(a_{t,i}|\mathbf{s}_{t,i})}$ is the importance ratio between the updated and reference policies. Unlike standard GRPO, where the advantage is computed from a fixed reward model, this formulation derives it from a continuously evolving mixture of reward terms. The policy thus receives feedback adapted to its learning stage, producing a smooth curriculum of optimization steps. This adaptive design enhances convergence stability and mitigates reward exploitation.

The Self-Paced GRPO framework unifies self-paced learning, adaptive reward adaptation, and group-relative optimization within a single formulation. By continuously aligning reward difficulty with model competence, it alleviates the saturation and instability of static rewards. The adaptive weighting of reward terms establishes a natural curriculum that sustains consistent learning dynamics. This formulation offers a general paradigm for evolving reward structures in generative policy optimization and provides a

foundation for scalable reinforcement alignment in high-dimensional generative tasks.

5. Experiment

5.1. Setup

We conduct experiments on Wan2.1-T2V with 1.3B and 14B variants [31], as well as HunyuanVideo [13]. Frozen Qwen2.5VL-7B and Qwen2.5VL-72B are employed as reward models. We compare against pretrained Wan2.1, Hunyuan backbones, and DanceGRPO as baselines.

Datasets. Our training is conducted on the 50k dataset released by DanceGRPO. For ablation studies, we randomly sampled 1.4k prompts from the iStock dataset [12] as our test set.

Evaluation Metrics. For quantitative evaluation, we adopt VBench [11], which assesses sixteen complementary dimensions to provide a comprehensive understanding of generative model performance. For ablation studies, we report four representative metrics, including VideoAlign, where VQ measures visual quality, MQ measures motion quality, and TA measures text alignment. In addition, we employ LAION [27] to evaluate video aesthetics.

5.2. Implementation details

Wan2.1-T2V-1.3B. Videos are sampled at $480 \times 832 \times 53$ frames at 15 fps. Reward gate thresholds are set to $\tau_I = \tau_{II} = 0.75$, with a learning rate of 5×10^{-6} and group size $G = 16$. Training is performed for 150 steps on 8 H100 GPUs.

Wan2.1-T2V-14B. Videos are sampled at $240 \times 416 \times 53$ frames at 15 fps. Reward gate thresholds are set to $\tau_I = 0.75$, $\tau_{II} = 0.73$, with a learning rate of 5×10^{-6} and group size $G = 16$. Training is performed for 220 steps on 16 H100 GPUs.

HunyuanVideo-T2V. Videos are sampled at $240 \times 416 \times 53$ frames at 15 fps. Reward gate thresholds are set to $\tau_I = 0.70$, $\tau_{II} = 0.68$, with a learning rate of 2×10^{-6} and group size $G = 16$. Training is performed for 100 steps on 16 H100 GPUs.

Self-Pace of Reward Model. We instantiate our progressive co-evolving design as a three-stage reward framework. Stage I optimizes visual quality, Stage II jointly optimizes visual quality and temporal consistency, and Stage III further incorporates text–video alignment. Following recent surveys on prompt engineering [2, 20, 35], we adopt progressive prompt design to gradually strengthen the reward capacity of Qwen models, akin to curriculum learning. Detailed prompt configurations are provided in the supplementary material.

Quantitative Evaluation and Ablation Study. We configure the sampling steps to 50 for Wan2.1-T2V-1.3B and Wan2.1-T2V-14B, with a resolution of $480 \times 832 \times 53$. For

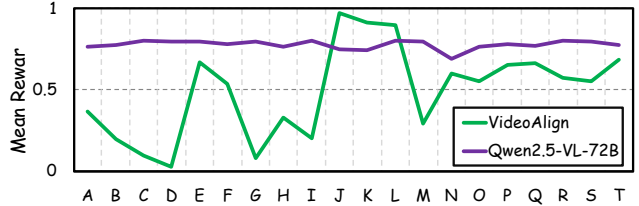


Figure 4. Reward preference analysis. We partition 2,000 real videos into 20 semantic categories, evaluate them using different reward models, and report the coefficient of variation of the mean scores across categories.

HunyuanVideo-T2V, we adopt 30 sampling steps under the same resolution setting.

Reward Model Preference Analyses. We randomly sampled 2k real-world videos with captions from the iStock dataset, grouped them into 10–20 clusters using the UMT5 [26] encoder, and scored each video with both VideoAlign and Qwen2.5VL-72B. Then, we computed the mean score and coefficient of variation κ within each cluster to quantify evaluation consistency.

5.3. Quantitative evaluation

Preference of Reward Model. As shown in Fig. 4, we compare the intra-cluster reward consistency of VideoAlign and Qwen2.5VL-72B across 20 semantic clusters. Since the evaluation is conducted on real-world videos, we naturally expect the visual quality between each semantic category to be comparable. VideoAlign, however, exhibits large variations in reward means across clusters and yields a coefficient of variation as high as 55.84, reflecting its inherent preference toward certain types of semantic content in videos. In contrast, Qwen2.5VL-72B produces more consistent scores within each class and maintains a much lower coefficient of variation of 3.4 across all cluster sizes, indicating stable and content-invariant evaluations. The analysis indicates that VideoAlign introduces category-specific bias in visual quality assessment, assigning disproportionate scores to semantically different videos of similar quality. Benefiting from stronger generalization capacity, larger models such as Qwen2.5VL-72B provide more consistent and unbiased reward feedbacks.

Wan2.1-1.3B-T2V. Table 1 presents the VBench evaluation of Wan1.3B. We compare our method with the untrained Wan1.3B and DanceGRPO as baselines. On the video quality side, our method achieves the best overall score, improving over the baseline in aesthetic quality, image quality, and dynamic degree. DanceGRPO, while competitive in dynamic degree and color, shows regressions in aesthetic and image quality, leading to a slightly lower quality score. On the semantic side, the benefits of larger reward modeling are more pronounced. Qwen2.5-VL-7B already im-

Table 1. Quantitative VBench results for Wan2.1-T2V-1.3B and Wan2.1-T2V-14B. For the 1.3B setting, we compare Wan and DanceGRPO (VideoAlign reward) with our **Self-Paced GRPO** using Qwen2.5VL-7B and Qwen2.5VL-72B rewards. For the 14B setting, we employ Qwen2.5VL-72B as the reward model, pretrained Wan14B as the baseline. The best score for each metric is shown in **bold**.

Metric	Wan1.3B	DanceGRPO	Ours		Wan14B	Ours
			Qwen2.5VL-7B	Qwen2.5VL-72B		Qwen2.5VL-72B
Aesthetic quality	60.92	58.99	60.97	62.64	65.33	60.68
Appearance style	20.41	20.70	20.45	20.48	21.35	21.62
Background consistency	96.80	96.83	96.83	96.49	98.36	98.74
Color	84.15	90.05	86.00	84.96	87.98	89.68
Dynamic degree	56.94	58.33	55.56	58.33	52.78	56.94
Human action	74.00	73.00	76.00	76.00	77.00	80.00
Image quality	67.65	66.61	67.63	68.49	68.03	68.91
Motion smoothness	98.32	98.15	98.28	98.23	98.35	98.30
Multiple objects	59.14	57.54	58.46	63.49	70.27	69.81
Object class	74.84	77.68	77.93	74.21	81.72	82.19
Overall consistency	23.63	23.68	23.76	23.67	25.08	25.17
Scene	22.38	25.79	20.49	25.94	32.12	30.67
Spatial relationship	68.08	62.89	72.78	72.00	74.97	79.06
Subject consistency	95.19	95.55	95.10	95.19	96.49	96.63
Temporal flickering	99.38	99.42	99.37	99.35	99.11	99.01
Temporal style	23.29	23.47	23.11	23.15	24.05	23.98
Quality score	83.15	82.81	83.02	83.53	84.03	84.59
Semantic score	65.31	66.06	66.26	66.94	71.18	72.08
Total score	79.58	79.46	79.67	80.22	81.46	82.09

proves object class by 77.93, color fidelity by 86.00, and spatial relationships by 72.78. Qwen2.5-VL-72B further enhances multiple-object handling 63.49 and scene alignment by 25.94, yielding the highest semantic score of 66.94. DanceGRPO, in contrast, excels in certain isolated metrics such as and scene alignment, but its gains are inconsistent and often accompanied by regressions in other semantic dimensions.

The results indicate that large-scale VLM reward models deliver more fine-grained perceptual supervision. Our method achieves this improvement by eliminating the need for fine-tuning on manually labeled datasets, thereby avoiding semantic bias toward specific video categories. Consequently, they provide more precise and unbiased reward signals. In addition, compared to smaller models such as Qwen2.5VL-7B, the larger Qwen2.5VL-72B benefits from greater parameter capacity and improved generalization. This results in more accurate reward signals and consequently more effective and stable training.

Wan2.1-14B-T2V.

As shown in Table 1, our method consistently surpasses the baseline across both quality and semantic dimensions on VBench. On the video quality side, it achieves clear gains in aesthetic quality, image fidelity, and dynamic degree, while also improving background and subject consistency. Although motion smoothness and temporal flickering show only marginal improvements, the overall quality

score increases, reflecting more stable and visually pleasing generations. On the semantic side, our method demonstrates stronger alignment with textual conditions, achieving higher accuracy in object class, human action, color fidelity, and spatial relationships. Consequently, the semantic score improves, indicating better content faithfulness. Despite slight declines in multiple-object handling and scene consistency, the overall total score advances.

We attribute these improvements to the progressive co-evolving reward mechanism. Unlike fixed reward models such as DanceGRPO with VideoAlign, our framework scales reward capacity with generation competence, providing stable and continuous feedback that supports sustainable training.

HunyuanVideo-T2V. As shown in Table 2, our method achieves consistent improvements over HunyuanVideo across a wide range of evaluation dimensions. On the visual side, it enhances appearance style, background consistency, and overall image fidelity, leading to generations that are more coherent and aesthetically pleasing. It also strengthens motion smoothness and reduces temporal flickering, contributing to stable dynamics and improved temporal quality. Beyond visual fidelity, our method demonstrates stronger handling of complex scenarios, including multiple-object interactions and spatial relationships, while maintaining subject consistency across frames. These gains collectively highlight the robustness of our Self-Paced GRPO

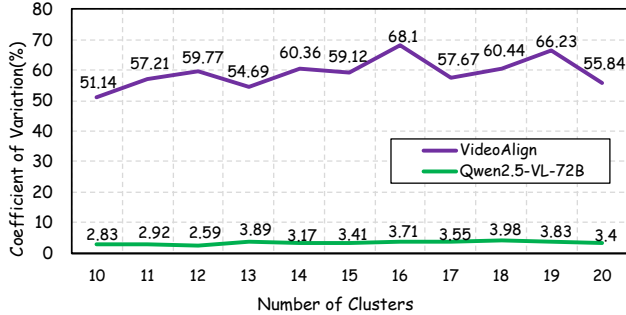


Figure 5. Ablation study: we further grouped 2,000 iStock [12] videos into 10–20 semantic clusters, using **VideoAlign** [20] and **Qwen2.5VL-72B** to evaluate them, and compute the coefficient of variation of the mean reward scores within each cluster.

framework. The results confirm that the proposed reward mechanism generalizes effectively, yielding reliable improvements when applied to different video generation backbones and ensuring balanced progress across both visual and semantic aspects of evaluation.

Table 2. Quantitative results on VBench for HunyuanVideo. We compare the Hunyuanvideo with our **Self-Paced GRPO** using Qwen-2.5VL-72B as reward model. The best performance for each metric is highlighted in **bold**.

Metric	Hunyuan	Ours+Hunyuan
Appearance style	19.95	20.26
Background consistency	96.45	96.85
Image quality	64.61	68.83
Motion smoothness	98.87	99.33
Multiple objects	69.51	71.42
Spatial relationship	67.55	69.84
Subject consistency	95.92	96.54
Temporal flickering	99.12	99.43
Temporal style	24.18	24.24

5.4. Ablation Study

(1) Comparison with Fewer Training Stages. To investigate whether our proposed progressive co-evolving reward mechanism outperforms simple one-stage and two-stage reward schemes, we conducted ablation experiments on Wan2.1-1.3B-T2V. As shown in Table 3, single-stage training, optimizing visual quality only, improves visual quality (VQ) and motion quality (MQ) but fails to substantially enhance text alignment (TA). Two-stage training (optimizing both visual quality and temporal consistency) further improves both VQ and MQ, yet still struggles to refine TA. In contrast, our method effectively mitigates this issue, achieving notable improvements in VQ, MQ, and TA, while also attaining the highest LAION score. We attribute

Table 3. Ablation study on Wan2.1-T2V-1.3B. We compare joint training, one-stage, and two-stage strategies with our method. Results are reported on VideoAlign metrics VQ, MQ, and TA, as well as the LAION aesthetic score.

Method	VideoAlign			LAION
	VQ↑	MQ↑	TA↑	Score↑
Wan2.1-1.3B-T2V	3.448	0.2911	-1.914	5.224
Joint train	3.366	0.3011	-1.077	5.222
One stage	3.481	0.3096	-1.502	5.249
Two stage	3.493	0.2973	-1.502	5.233
Ours	3.501	0.3090	-0.7114	5.252

this improvement to the increased reward capacity enabled by multi-stage design. By progressively expanding the reward model, our framework delivers feedback that is harder to be hacked, resulting in more robust and effective training. These results highlight the importance of progressive multi-stage reward feedback for balanced gains across visual, temporal, and semantic dimensions.

(2) Comparison with Direct Joint-training. To assess the effectiveness of our co-evolving reward design, we conduct ablation experiments comparing direct joint-training with our progressive approach. In the joint training setting, the three reward signals are aggregated into a single score, which is then used for advantage estimation and loss optimization. While this method improves over the baseline (e.g., VQ 3.481 vs. 3.448, MQ 0.3011 vs. 0.2911, TA -1.077 vs. -1.914), it consistently underperforms our progressive design (VQ 3.501, MQ 0.3090, TA -0.7114 , Laion 5.252). We attribute this gap to conflicting optimization directions among different rewards, which cause gradients to deviate from enhancing overall video quality. These results highlight that progressive reward mechanism provides more stable and effective optimization than simply aggregating reward scores in a joint single stage.

Cluster-wise Reward Preference Analysis. To further investigate the robustness of reward feedback across semantic categories, we conduct an ablation study by partitioning $2k$ videos into $10-20$ clusters and measuring the coefficient of variation κ for each model. As shown in Fig. 5, VideoAlign exhibits substantial fluctuations in κ , ranging from 51.14% to 68.10%, indicating a strong bias toward specific video types and inconsistent reward behavior across clusters. In contrast, our Qwen2.5-VL-72B reward model maintains remarkably stable κ values between 2.59% and 3.98%, demonstrating consistent reward assignment regardless of clustering granularity. The ablation results indicate that VideoAlign exhibits a preference for specific content videos, and this bias does not disappear with changes in the number of video clusters.

Prompt: A couple in formal evening wear going home get caught in a heavy downpour with umbrellas, racking focus

Wan2.1-14B-T2V



Ours



Prompt: A boat sailing leisurely along the Seine River with the Eiffel Tower in background by Hokusai.

Wan2.1-14B-T2V



Ours



Prompt: Vibrant urban street food scene, colorful hot dog cart with mascot sign. Vendor in chef's hat grilling hot dogs, assistant serving condiments, customers lining up. Close-up of hot dogs with mustard, ketchup, onions. Warm golden sunlight, lively crowd atmosphere.

Wan2.1-14B-T2V



Ours



Figure 6. Qualitative comparison between Wan2.1-T2V-14B and our fine-tuned model. Top: baseline Wan2.1-T2V-14B results. Bottom: outputs from our fine-tuned model.

5.5. Qualitative Research

Visual Comparison. To complement the quantitative results, we conduct qualitative case studies to provide intuitive evidence of our method’s advantages. By visually comparing generated samples under different settings, we highlight improvements in visual fidelity, temporal coherence, and semantic alignment, qualities not always fully captured by numerical metrics. As shown in Fig. 6, in case (1), our method prevents incorrect umbrella generation and achieves better image composition. In case (2), it produces higher visual quality with more vivid colors. In case (3), it generates the correct visual theme, demonstrating improved semantic consistency. Overall, the qualitative analysis demonstrates enhanced visual fidelity and stronger semantic alignment with the text.

6. Conclusion

In this paper, we introduced Self-Paced GRPO, a competence-aware extension of GRPO that progressively adapts reward feedback to generation ability. Self-Paced GRPO consistently outperforms static reward baselines across diverse video generation backbones, achieving balanced improvements in visual quality, temporal coherence, and text–video alignment. Beyond empirical gains, our framework establishes a paradigm that integrates adaptive rewards with reinforcement learning. We believe this work opens new directions for post-training optimization in generative video models and will inspire future research on curriculum-based reward design, multi-modal alignment, and scalable reinforcement learning for high-dimensional generation tasks.

References

- [1] Mido Assran, Adrien Bardes, David Fan, Quentin Garrido, Russell Howes, Matthew Muckley, Ammar Rizvi, Claire Roberts, Koustuv Sinha, Artem Zhohus, et al. V-jepa 2: Self-supervised video models enable understanding, prediction and planning. *arXiv preprint arXiv:2506.09985*, 2025. 2
- [2] Huilin Deng, Ding Zou, Rui Ma, Hongchen Luo, Yang Cao, and Yu Kang. Boosting the generalization and reasoning of vision language models with curriculum reinforcement learning. *arXiv preprint arXiv:2503.07065*, 2025. 5, 1
- [3] Kenji Doya. Reinforcement learning in continuous time and space. *Neural computation*, 12(1):219–245, 2000. 2
- [4] Xueji Fang, Liyuan Ma, Zhiyang Chen, Mingyuan Zhou, and Guo-jun Qi. Inflvg: Reinforce inference-time consistent long video generation with grpo. *arXiv preprint arXiv:2505.17574*, 2025. 1, 2
- [5] Yuxin Fang, Bencheng Liao, Xinggang Wang, Jiemin Fang, Jiyang Qi, Rui Wu, Jianwei Niu, and Wenyu Liu. You only look at one sequence: Rethinking transformer in vision through object detection. *Advances in Neural Information Processing Systems*, 34:26183–26197, 2021. 2
- [6] Hiroki Furuta, Heiga Zen, Dale Schuurmans, Aleksandra Faust, Yutaka Matsuo, Percy Liang, and Sherry Yang. Improving dynamic object interactions in text-to-video generation with ai feedback. *arXiv preprint arXiv:2412.02617*, 2024. 2
- [7] Uri Hasson, Janice Chen, and Christopher J Honey. Hierarchical process memory: memory as an integral component of information processing. *Trends in cognitive sciences*, 19(6):304–313, 2015. 2
- [8] Xiaoxuan He, Siming Fu, Yuke Zhao, Wanli Li, Jian Yang, Dacheng Yin, Fengyun Rao, and Bo Zhang. Tempflow-grpo: When timing matters for grpo in flow models. *arXiv preprint arXiv:2508.04324*, 2025. 1
- [9] Patrik O Hoyer. Non-negative matrix factorization with sparseness constraints. *Journal of machine learning research*, 5(Nov):1457–1469, 2004. 3
- [10] Panwen Hu, Nan Xiao, Feifei Li, Yongquan Chen, and Rui Huang. A reinforcement learning-based automatic video editing method using pre-trained vision-language model. In *Proceedings of the 31st ACM International Conference on Multimedia*, pages 6441–6450, 2023. 2
- [11] Ziqi Huang, Yanan He, Jiashuo Yu, Fan Zhang, Chenyang Si, Yuming Jiang, Yuanhan Zhang, Tianxing Wu, Qingyang Jin, Nattapol Chanpaisit, et al. Vbench: Comprehensive benchmark suite for video generative models. In *Proceedings of the IEEE/CVF Conference on Computer Vision and Pattern Recognition*, pages 21807–21818, 2024. 5
- [12] iStock. istock video dataset. <https://www.istockphoto.com/videos>, 2025. Accessed: Oct. 17, 2025. 5, 7
- [13] Weijie Kong, Qi Tian, Zijian Zhang, Rox Min, Zuozhuo Dai, Jin Zhou, Jiangfeng Xiong, Xin Li, Bo Wu, Jianwei Zhang, et al. Hunyuanvideo: A systematic framework for large video generative models. *arXiv preprint arXiv:2412.03603*, 2024. 5
- [14] Patricia K Kuhl. Early language acquisition: cracking the speech code. *Nature reviews neuroscience*, 5(11):831–843, 2004. 2
- [15] Jiachen Li, Qian Long, Jian Zheng, Xiaofeng Gao, Robinson Piramuthu, Wenhui Chen, and William Yang Wang. T2v-turbo-v2: Enhancing video generation model post-training through data, reward, and conditional guidance design. *arXiv preprint arXiv:2410.05677*, 2024. 1
- [16] Junzhe Li, Yutao Cui, Tao Huang, Yinping Ma, Chun Fan, Miles Yang, and Zhao Zhong. Mixgrpo: Unlocking flow-based grpo efficiency with mixed ode-sde. *arXiv preprint arXiv:2507.21802*, 2025. 1
- [17] Rui Li and Dong Liu. Spatial-then-temporal self-supervised learning for video correspondence. In *Proceedings of the IEEE/CVF Conference on Computer Vision and Pattern Recognition*, pages 2279–2288, 2023. 2
- [18] Ji Lin, Hongxu Yin, Wei Ping, Pavlo Molchanov, Mohammad Shoeybi, and Song Han. Vila: On pre-training for visual language models. In *Proceedings of the IEEE/CVF conference on computer vision and pattern recognition*, pages 26689–26699, 2024. 2
- [19] Jie Liu, Gongye Liu, Jiajun Liang, Yangguang Li, Jiaheng Liu, Xintao Wang, Pengfei Wan, Di Zhang, and Wanli Ouyang. Flow-grpo: Training flow matching models via on-line rl. *arXiv preprint arXiv:2505.05470*, 2025. 1, 2
- [20] Jie Liu, Gongye Liu, Jiajun Liang, Ziyang Yuan, Xiaokun Liu, Mingwu Zheng, Xiele Wu, Qiulin Wang, Menghan Xia, Xintao Wang, et al. Improving video generation with human feedback. *arXiv preprint arXiv:2501.13918*, 2025. 1, 5, 7
- [21] Yang Liu, Qianqian Xu, Peisong Wen, Siran Dai, and Qingming Huang. When the future becomes the past: Taming temporal correspondence for self-supervised video representation learning. In *Proceedings of the Computer Vision and Pattern Recognition Conference*, pages 24033–24044, 2025. 2
- [22] Yang Luo, Xuanlei Zhao, Mengzhao Chen, Kaipeng Zhang, Wenqi Shao, Kai Wang, Zhangyang Wang, and Yang You. Enhance-a-video: Better generated video for free. *arXiv preprint arXiv:2502.07508*, 2025. 2
- [23] Yecheng Jason Ma, Vikash Kumar, Amy Zhang, Osbert Bastani, and Dinesh Jayaraman. Liv: Language-image representations and rewards for robotic control. In *International Conference on Machine Learning*, pages 23301–23320. PMLR, 2023. 2
- [24] Mihir Prabhudesai, Russell Mendonca, Zheyang Qin, Katearina Fragkiadaki, and Deepak Pathak. Video diffusion alignment via reward gradients. *arXiv preprint arXiv:2407.08737*, 2024. 2
- [25] Alec Radford, Jong Wook Kim, Chris Hallacy, Aditya Ramesh, Gabriel Goh, Sandhini Agarwal, Girish Sastry, Amanda Askell, Pamela Mishkin, Jack Clark, et al. Learning transferable visual models from natural language supervision. In *International conference on machine learning*, pages 8748–8763. PmLR, 2021. 2
- [26] Colin Raffel, Noam Shazeer, Adam Roberts, Katherine Lee, Sharan Narang, Michael Matena, Yanqi Zhou, Wei Li, and Peter J. Liu. Exploring the limits of transfer learn-

- ing with a unified text-to-text transformer. *arXiv preprint arXiv:1910.10683*, 2020. 5
- [27] Christoph Schuhmann, Romain Beaumont, Richard Vencu, Cade Gordon, Ross Wightman, Mehdi Cherti, Theo Coombes, Aarush Katta, Clayton Mullis, Mitchell Wortsman, et al. Laion-5b: An open large-scale dataset for training next generation image-text models. *Advances in neural information processing systems*, 35:25278–25294, 2022. 2, 5
- [28] Wolfram Schultz. Predictive reward signal of dopamine neurons. *Journal of neurophysiology*, 1998. 2
- [29] Zhihong Shao, Peiyi Wang, Qihao Zhu, Runxin Xu, Junxiao Song, Xiao Bi, Haowei Zhang, Mingchuan Zhang, YK Li, Yang Wu, et al. Deepseekmath: Pushing the limits of mathematical reasoning in open language models. *arXiv preprint arXiv:2402.03300*, 2024. 2
- [30] Zhan Tong, Yibing Song, Jue Wang, and Limin Wang. Videomae: Masked autoencoders are data-efficient learners for self-supervised video pre-training. *Advances in neural information processing systems*, 35:10078–10093, 2022. 2
- [31] Team Wan, Ang Wang, Baole Ai, Bin Wen, Chaojie Mao, Chen-Wei Xie, Di Chen, Feiwu Yu, Haiming Zhao, Jianxiao Yang, et al. Wan: Open and advanced large-scale video generative models. *arXiv preprint arXiv:2503.20314*, 2025. 5
- [32] Xiaoshi Wu, Yiming Hao, Keqiang Sun, Yixiong Chen, Feng Zhu, Rui Zhao, and Hongsheng Li. Human preference score v2: A solid benchmark for evaluating human preferences of text-to-image synthesis. *arXiv preprint arXiv:2306.09341*, 2023. 2
- [33] Jiazheng Xu, Yu Huang, Jiale Cheng, Yuanming Yang, Jiajun Xu, Yuan Wang, Wenbo Duan, Shen Yang, Qunlin Jin, Shurun Li, et al. Visionreward: Fine-grained multi-dimensional human preference learning for image and video generation. *arXiv preprint arXiv:2412.21059*, 2024. 1
- [34] Zeyue Xue, Jie Wu, Yu Gao, Fangyuan Kong, Lingting Zhu, Mengzhao Chen, Zhiheng Liu, Wei Liu, Qiushan Guo, Weilin Huang, et al. Dancegrpo: Unleashing grpo on visual generation. *arXiv preprint arXiv:2505.07818*, 2025. 1, 2
- [35] Hongji Yang, Yucheng Zhou, Wencheng Han, and Jianbing Shen. Self-rewarding large vision-language models for optimizing prompts in text-to-image generation. *arXiv preprint arXiv:2505.16763*, 2025. 5, 1
- [36] Xiaomeng Yang, Zhiyu Tan, and Hao Li. Ipo: Iterative preference optimization for text-to-video generation. *arXiv preprint arXiv:2502.02088*, 2025. 2

Growing with the Generator: Self-paced GRPO for Video Generation

Supplementary Material

Due to space limitations in the main paper, this supplementary document provides additional details and analysis. The contents are organized as follows:

- **Training Details.** We first describe the training configurations and hyperparameters used in our experiments in Sec. A.
- **VLM Preference Analysis.** We provide further analysis on the content-specific biases exhibited by VLM-based reward models. Additionally, we present the input template used for reward evaluation in Sec. B.
- **Extended Qualitative Comparisons.** We include more qualitative examples comparing Wan2.1-T2V-14B and Self-Paced GRPO, highlighting the superior performance of our proposed method in terms of semantic fidelity and visual quality in Sec. C.

A. Training Details.

Experimental Setup. A batch size of 8 is adopted for Wan2.1-T2V-1.3B and 16 for Wan2.1-T2V-14B, with gradient accumulation set to 4. The optimizer is configured with a learning rate weight decay of 0.0001 and a maximum gradient norm of 1.0, without warmup. SDE sampling is conducted with 16 steps, using a noise strength parameter of $\eta = 0.5$ and a sampling time step shift of 5.0. Each iteration produces 16 samples under a best-of- $n = 8$ strategy. The overall configuration further employs a training timestep fraction of 0.6 to ensure effectiveness, consistent noise initialization, a clipping range of 1×10^{-4} for the importance ratio $\rho_{t,i}$, and an adversarial clipping maximum of 5.0. In addition, gradient checkpointing, sequential classifier-free guidance (CFG), and bf16 mixed-precision training are utilized to improve memory efficiency and training stability.

Self-Pace for Reward Model. Several recent studies provide strong evidence that imposing stricter and more structured prompts enhances the supervisory capacity of large VLMs such as Qwen2.5-VL-72B when used as reward models. [20, 35] show that prompt optimization directly improves the reliability of reward signals in text-to-image generation. The VideoGen-RewardBench benchmark further indicates that fine-grained and multi-stage prompts enable VLM-based reward models to capture subtle quality differences in generated videos, thereby improving alignment with human preferences. In addition, curriculum learning approaches for reward modeling [2] confirm that gradually increasing prompt complexity strengthens the discriminative power of reward models, allowing them to deliver more stable and informative supervision. Collectively, these findings support the design choice: progressively stricter

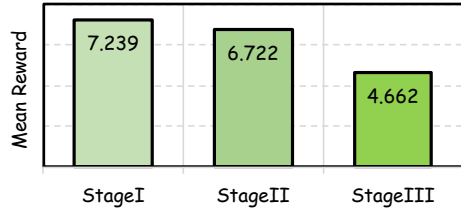


Figure 7. Self-paced Reward Model: Different stages of VLMs are employed to evaluate the outputs of SDE sampling. The results indicate that more complex prompts enable the VLM-based reward model to provide stronger supervisory signals.

prompts allow VLMs to serve as a more effective self-paced reward model, providing higher-quality guidance during GRPO training.

In addition to the reported results, 1k videos were sampled using the same SDE strategy as employed during training. Each video was evaluated under the three designed stages. The average scores were then computed, as shown in Fig. 7. With increasing prompt complexity, Qwen2.5-VL-72B was able to produce more rigorous evaluations. This analysis demonstrates that stricter prompts enhance the model’s ability to deliver consistent and discriminative supervision.

Stage Threshold. In the self-paced GRPO framework, stage thresholds are critical for weighting different phases. Thresholds selected purely by heuristics are considered inappropriate, as they may introduce bias and instability. To obtain reliable values, Stage I, Stage II, and Stage III were separately trained for 50 steps each, and the corresponding reward improvements were recorded. The thresholds were then set to 0.7 times the observed increased reward. This design ensures that the thresholds are grounded in empirical evidence and provide balanced supervision across stages.

Reward cruves. To validate the effectiveness of the reinforcement learning method, the reward curve of Stage I during training is presented. Following DanceGRPO, a smoothing window was applied to plot the curve. As shown in Fig. 10, the reward exhibits a stable upward trend, indicating the effectiveness of the training process.

Input Template of Reward Model. As illustrated in Fig. 14, the Reward Model’s Input Template is presented in detail. It is structured into three stages, Visual Quality, Temporal Smoothness, and Text Alignment—each comprising multiple sub-dimensions. Together, these elements constitute the complete input template.

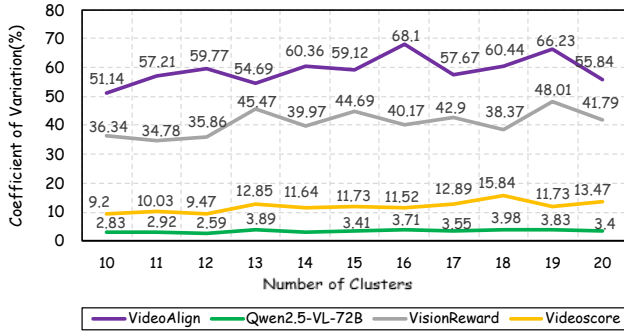


Figure 8. Bias of Other VLMs on Real-World videos. The results suggest that other VLM-based Reward Models are biased toward certain types of video content.

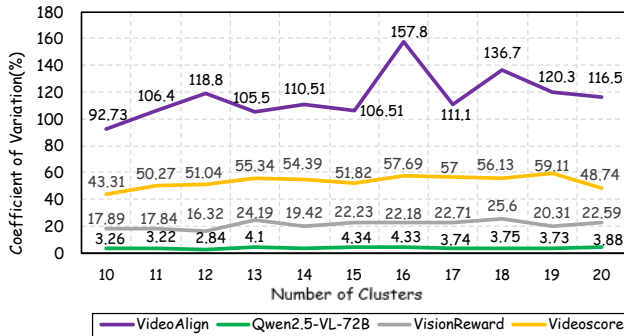


Figure 9. Bias of Other VLMs on Generated Videos. The results show that VLM-based Reward Models also exhibit specific content preferences with generating videos. Moreover, VLM-based Reward Models reveal stronger content bias on generated videos than real-world videos.

B. Preference of VLMs-based Reward Models.

Bias of VLMs on Real-world Videos. To investigate whether VLM-based reward models exhibit content-specific preferences beyond VideoAlign, an empirical study was conducted. In particular, VideoAlign, VisionReward, VideoScore, and Qwen2.5-VL-72B were compared to analyze potential biases across different types of generated videos. The results, summarized in Fig. 8, reveal distinct preference patterns among these models, underscoring the importance of model choice in reward-based evaluation.

Bias of VLMs on Generated Videos. To examine whether VLM-based reward models exhibit similar content preferences in generated videos, experiments were conducted on a set of 2k generated samples. As shown in Fig. 9, more pronounced content biases were observed across four different VLMs compared to real-world videos.

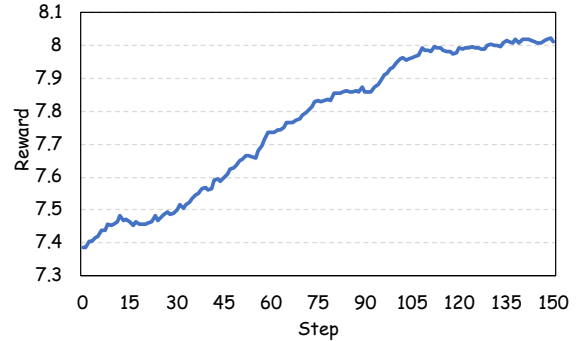


Figure 10. Reward curves. The steadily increasing trend during training indicates that our reinforcement learning procedure is stable and effective.

C. Additional Qualitative Study.

Additional qualitative comparisons are provided to highlight the advantages of the proposed approach.

Less Structural Inconsistencies. As shown in Fig. 11, in case A, our model successfully generates the correct facial features of a sheep, whereas Wan2.1-T2V-14B fails to produce them. In case B, our model generates a sliced lemon, which is consistent with real-world constraints, since lemon juice cannot be extracted without cutting. In cases C and D, our model produces anatomically correct yoga poses, while Wan fails to generate valid limb structures.

Better Visual Quality As shown in Fig. 12, in case E, the seaside environment surrounding the woman appears more aesthetically pleasing, with refined composition. In case F, the boy’s umbrella exhibits richer details and more intricate patterns. In case G, the cutting board contains additional objects, and the presence of green leaves makes the scene more vivid and colorful. In case H, the woman’s background becomes less monotonous and shows more dynamic variation.

Better Alignment with Reality As shown in Fig. 13, in case H, our model generates the scientist and computer with accurate relative positioning, while Wan produces a person operating an invisible computer, which violates physical plausibility. In case I, our model avoids abrupt color changes of the balls, whereas Wan generates a transition from one blue and one red ball to two red balls.

Better Text Alignment. As shown in Fig. 13, in case J, our model produces correct text alignment with a single man as specified in the prompt, while Wan incorrectly generates two men. In case K, the prompt requires two dogs riding an electric scooter. Our model correctly generates dogs riding the scooter, whereas Wan produces a human rider.

Prompt: A sheep walking on the grass, peacefully.

Wan2.1-14B-T2V



A

Ours



Prompt: Squeezing zesty lemon into water.

Wan2.1-14B-T2V



B

Ours



Prompt: a woman is performing leg exercises on a yoga mat in a brightly lit studio.

Wan2.1-14B-T2V



C

Ours



Prompt: a woman is practicing yoga in a spacious room with large windows.

Wan2.1-14B-T2V



D

Ours



Figure 11. Examples of generated results with fewer structural inconsistencies.

Prompt: a woman in a pink dress walks along a sandy beach during sunset.

Wan2.1-14B-T2V



E

Ours



Prompt: A whimsical illustration in a vintage comic book style, a purple umbrella with intricate floral patterns and metallic accents, standing alone on a cobblestone street at sunset.....

Wan2.1-14B-T2V



F

Ours



Prompt: a butter knife smears peanut butter on a slice of bread.

Wan2.1-14B-T2V



G

Ours



Prompt: a woman is walking along the sea.

Wan2.1-14B-T2V



H

Ours



Figure 12. Examples of generated results with better visual quality.

Prompt: a focused office worker operates a computer in a modern tech environment.

Wan2.1-14B-T2V



H

Ours



Prompt: a red ball and a blue ball fall from a height hits the ground and bounces back up.

Wan2.1-14B-T2V



I

Ours



Prompt: a man is standing on an elliptical machine, reading some papers while occasionally looking up and speaking into a microphone.

Wan2.1-14B-T2V



J

Ours



Prompt: two dogs are riding on motorized skateboards in an open area.

Wan2.1-14B-T2V



K

Ours



Figure 13. Examples of generated results with better real-world alignment and text alignment.

Input Template for Reward Model

[VIDEO] You are an expert in judging {*evaluation dims*} of AI-generated videos.

Here is the caption of the video:

"{*text_prompt*}"

please watch the frames of a given video and see the text prompt for generating the video, then give scores based on its {*evaluation dims*}.

Output a float number from 1.0 to 10.0 for this dimension,

the higher the number is, the better the video performs in that sub-score,

the lowest 1.0 means Bad, the highest 10.0 means Perfect/Real (the video is like a real video)

Output only ONE float number between 1.00 and 10.00 (e.g., 5.80) that represents the stage score.

StageI: Assess how well the video matches the textual prompt across the following sub-dimensions:

Visual Quality

Visual Quality:

Evaluate the overall visual quality of the video, with a focus on static factors. The following sub-dimensions should be considered:

- **Reasonableness:** The video should not contain any significant biological or logical errors, such as abnormal body structures or nonsensical environmental setups.

- **Clarity:** Evaluate the sharpness and visibility of the video. The image should be clear and easy to interpret, with no blurring or indistinct areas.

- **Detail Richness:** Consider the level of detail in textures, materials, lighting, and other visual elements (e.g., hair, clothing, shadows).

- **Aesthetic and Creativity:** Assess the artistic aspects of the video, including the color scheme, composition, atmosphere, depth of field, and the overall creative appeal. The scene should convey a sense of harmony and balance.

- **Safety:** The video should not contain harmful or inappropriate content, such as political, violent, or adult material. If such content is present, the image quality and satisfaction score should be the lowest possible.

StageII: Assess how well the video matches the textual prompt across the following sub-dimensions:

Temporal Smoothness, while also take into account **Visual Quality**.

Temporal Smoothness:

Assess the dynamic aspects of the video, with a focus on dynamic factors. Consider the following sub-dimensions:

- **Stability:** Evaluate the continuity and stability between frames. There should be no sudden, unnatural jumps, and the video should maintain stable attributes (e.g., no fluctuating colors, textures, or missing body parts).

- **Naturalness:** The movement should align with physical laws and be realistic. For example, clothing should flow naturally with motion, and facial expressions should change appropriately (e.g., blinking, mouth movements).

- **Aesthetic Quality:** The movement should be smooth and fluid. The transitions between different motions or camera angles should be seamless, and the overall dynamic feel should be visually pleasing.

- **Fusion:** Ensure that elements in motion (e.g., edges of the subject, hair, clothing) blend naturally with the background, without obvious artifacts or the feeling of cut-and-paste effects.

- **Clarity of Motion:** The video should be clear and smooth in motion. Pay ow score for motion quality. attention to any areas where the video might have blurry or unsteady sections that hinder visual continuity.

- **Amplitude:** If the video is largely static or has little movement, assign a low score for motion quality.

StageIII: Assess how well the video matches the textual prompt across the following sub-dimensions:

Text Alignment, while also take into account **Visual Quality** and **Temporal Smoothness**.

Text Alignment: - **Subject Relevance** Evaluate how accurately the subject(s) in the video (e.g., person, animal, object) align with the textual description. The subject should match the description in terms of number, appearance, and behavior.

- **Motion Relevance:** Evaluate if the dynamic actions (e.g., gestures, posture, facial expressions like talking or blinking) align with the described prompt. The motion should match the prompt in terms of type, scale, and direction.

- **Environment Relevance:** Assess whether the background and scene fit the prompt. This includes checking if real-world locations or scenes are accurately represented, though some stylistic adaptation is acceptable.

- **Style Relevance:** If the prompt specifies a particular artistic or stylistic style, evaluate how well the video adheres to this style.

- **Camera Movement Relevance:** Check if the camera movements (e.g., following the subject, focus shifts) are consistent with the expected behavior from the prompt.

Figure 14. Detailed illustration of input template of reward model.